Lowland Technology International 2016; 17 (4): 207-214
International Association of Lowland Technology (IALT): ISSN 1344-9656

Research Paper

Evaluation of rainfall erosivity and impact forces using strain gauges

K. Vilayvong [1], N. Yasufuku [2] and R. Ishikura [3]

ARTICLE INFORMATION

Article history:

Received: 26 November 2015
Received in revised form: 12 February 2016
Accepted: 25 Feb 2016
Published: March 2016

Keywords:

Drop diameter
Impact force
Miniature strain gauge
Rainfall erosivity
Terminal velocity

ABSTRACT

Rainfall erosivity and impact forces are key meteorological parameters for predicting rainfall-induced hazards and disasters. Erosivity of rainfall is widely indicated by its kinetic energy or momentum that is widely derived from drop diameters or drop size distribution and velocity of raindrops. Raindrop velocity and impact forces describe the rainfall erosivity dissipated to impacting surface. These parameters are not commonly evaluated and available in practice due to cost and capability of measuring instruments. A strain gauge-based device was developed for automatic and continuous measurement of the parameters in laboratory. The strain sensor, with the aid of a portable, dynamic, and high frequency data acquisition, was calibrated to capture the falling velocity of a 4.00 mm diameter waterdrop with varying heights. Results of the falling velocities of a waterdrop against heights in this study showed a close agreement with results from literature data and equations for the falling velocity and its impact force of a waterdrop were derived. In addition, results of using the equations to derive terminal velocities and impact forces as a function of drop diameters were presented.

1. Introduction

Rainfall-related hazards and disasters are typically observed in both lowland and highland areas. Problems associated with the hazards and disasters are soil erosion, land degradation, water quality, sedimentation, landslide, slope instability, flood, embankment failure and environmental pollution. Aftermaths of the hazards and disasters yield the danger to human lives, disruption to economic flow and damage to infrastructural properties. In recent years, it is likely that the frequency of heavy and extreme rainfall is increased over many areas of the globe (IPCC, 2012). Therefore, the change shifts the characteristics of surface and subsurface water movement that will influence soil erosion characteristics (Nearing et. al., 2004; Yasufuku et at., 2015), landslide and slope instability (Crozier, 2010; Rahardjo et al., 2014), water quality and environmental pollution (Bates et al., 2008; Cousino et al., 2015,), and flood and sedimentation (Shrestha et al, 2013; Camici et al., 2014).

Soil detachment of surface soil due to splash erosion is triggered by the erosive and destructive forces of rainfall. It was recognized that the capacity of rain to detach and transport soil particles is a function of rainfall energy or rainfall erosivity. The rainfall erosivity is indicated by the degree of impact force, stress, kinetic

[1] Corresponding author, PhD Student, Dept of Civil and Structural Engineering, Kyushu University, Fukuoka 813-0395, JAPAN, sangsinsay@gmail.com
[2] Professor, IALT member, Dept of Civil and Structural Engineering, Kyushu University, Fukuoka 813-0395, JAPAN, yasufuku@civil.kyushu-u.ac.jp
[3] Assistant Professor, IALT member, Dept of Civil and Structural Engineering, Kyushu University, Fukuoka 813-0395, JAPAN, ishikura@civil.kyushu-u.ac.jp
Note: Discussion on this paper is open until September 2016.

energy or momentum of a single raindrop and is a function of the drop size or drop size distribution (DSD), shape, and terminal velocity (Sharma, 1996; Goebes et. at., 2014). In Universal Soil Loss Equation (USLE), a factor R is a common representative of the rainfall erosivity. It is the product of rainfall energy and its maximum 30 minute rainfall intensity (Wischmeier and Smith, 1978). Direct determination of the rainfall kinetic energy is difficult and cumbersome as instruments that possess the capability of continuous measurement and high frequency of data sampling and time in unit of microsecond are required. In addition, drop size distribution (DSD) of a storm with corresponding terminal velocities of individual drop size varies geographically, spatially and temporally.

In soil erosion, simple and portable measuring instruments with low cost, low power consumption and low maintenance with high reliability and accuracy are desirable. Some researchers measure rainfall erosivity by using piezoelectric transducers with aid of signal amplifier or a digital oscilloscope to convert drop impact signal at high frequency and records time in microsecond (Nearing and Bradford, 1986; Jayawardena and Rezaur, 2000; Abd Elbasit et al., 2011). The more sophisticated and expensive methods for obtaining the rainfall erosivity is a laser-based disdrometer (Carollo and Ferro, 2014; Meshesha, et al., 2015). Some researchers (Hinkle, 1989; Nearing et al. 1986) employed empirically based impact sensors to indirectly obtain the output signal of sensors that varies with drop sizes and velocities to study waterdrop impact force, kinetic energy and momentum. Despite several methods are existed, the measurement of rainfall erosivity and destructive impact force is still limited.

Measurement of soil erosion and the discharged sediment sizes subjected to rainfall erosivity is a challenge because of information on drop diameters or DSD and other necessary meteorological or hydrological data such as terminal velocity is not widely available in practice. Therefore, a novel instrument is developed. The objective of this study is an attempt to fabricate, calibrate, and validate a miniature strain gauge device with configuration of a cantilever strip to measure the output of the strain gauges. The output is then used to directly derive velocity, impact force, kinetic energy, and momentum of a waterdrop under consideration of user-friendly, portable, low cost, direct and continuous measurement with high reliability and accuracy.

2. Materials and methods

2.1 Rainfall simulator

A single drop rainfall simulator using a hypodermic needle was used to form a water droplet. The needle is connected to a Marriott bottle filled with distilled water through a tube. Water flow or volume can be regulated by a mechanical flow meter and a regulator with readout mark. Volume of water can be adjusted according to desired frequency and intensity.

2.2 Fabrication of strain gauge-based device

Strain gauge offer benefit features such as small space for installation, good frequency response for rapid fluctuations of stresses, strains or forces, simultaneous measurement of multiple points a remote measurement, and electrical output for easy data processing. In comparison to piezoelectric sensor, strain gauge offers a better stability and linearity for long term data acquisition and application. Some limitations of strain gauges include temperature, fatigue, amount of strain, and measuring environment.

Figure 1 shows the schematic diagram of the instrument setup. Strain gauge based measurement system consists of two miniature strain gauges, a cantilever strip, a dynamic strain data recorder and analyzer, and a personal computer. Two miniature strain gauges were mounted on the cantilever strip using adhesive epoxy; one on the upper side and one is bottom side. The strain analog signal is amplified, output and recorded to an external recorder. The analog signal was then digitized to dynamically digital output using the dynamic strain data acquisition. The continuous strain data was recorded internally before being analyzing and transferring to a computer.

2.3 Rainfall impact pad

Rainfall impact pad is fabricated such that the pad could receive both a single drop and a number of waterdrops simultaneously can be applicable to both indoor and outdoor rainfall experiments and actual rainfall. The pad has a concave umbrella shape made of aluminum sheet derived from a discarded soft drink can. The pad is connected with a smooth and frictionless pin through a small drilled hole to connect to the loading point on the cantilever tip. The light weight pad is designed to allow minimum deflection of the cantilever tip when loaded with the pad. Thus, force transferred from momentum of rainfall can be transferred through the pin and the force acting on the cantilever is a point load or concentrated load. The impact force can be readily obtained by using the results of deflection at the loading point on the cantilever strip.

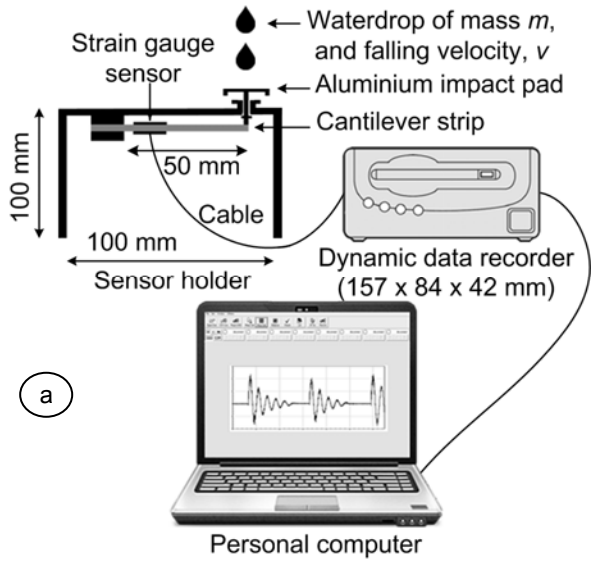

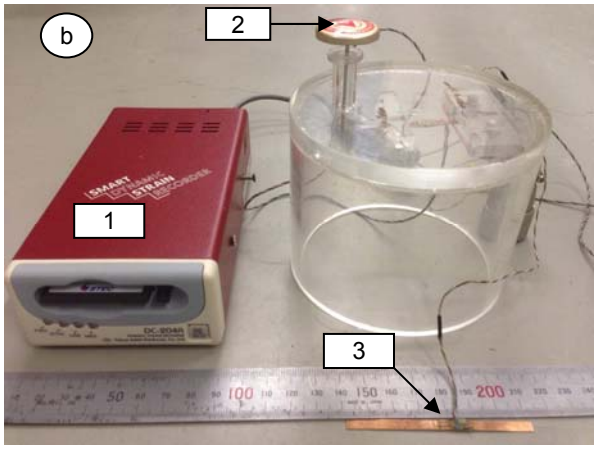

Fig. 1. Schematic diagram of instrument setup: a) setup configuration of the measurement system, b) photographs of the setup device: 1) dynamic strain recorder/data logger, 2) rainfall impact pad, 3) Ni-Cu cantilever strip with strain gauges.

2.4 Data acquisition and analysis

A commercially available 4-channel digital strain gauge recorder with an internal data compact flash memory of 2 Gbyte capacity (Model DC-204/DC-204Ra from Tokyo Sokki Kenkyujo Co., Ltd) was employed. The recorder has a small and portable physical dimension of 157 mm (length) x 84 mm (width) x 42 mm (height) and mass of 500 g. It can also be supplied by either AC power (10-16 volts and Maximum 0.4A) or A3 battery DC power (in the range of 1-20 volts).

It has options for measuring a dynamic strain, DC voltage, and thermocouple with frequency response up to 10 kHz and maximum data sampling speed of 5 μs. The recorded strain data of the strain gauge in the data recorder can be accessed via a USB interface cable using a personal computer. Dynamic strain recorder measurement software was used to analyze the data.

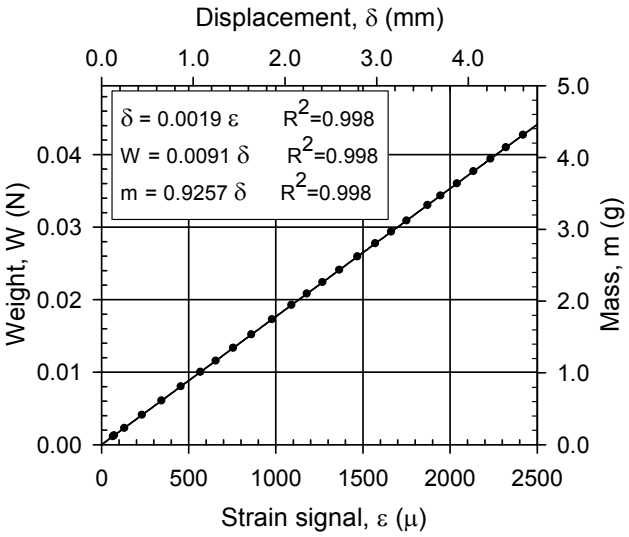

Fig. 2. Calibration and relationship of strain gauge output.

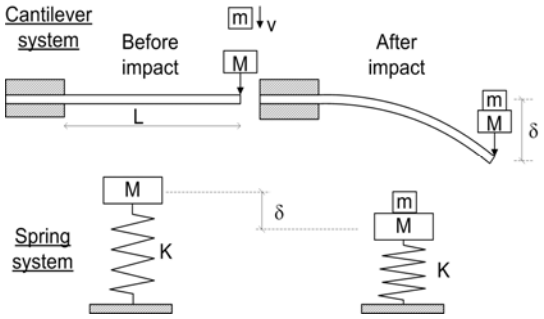

Fig. 3. Free body diagram for cantilever and spring systems.

2.5 Calibration of the strain gauge-based cantilever strip

Calibration was conducted to establish the relationship between strain gauge output signal with tip deflection of the cantilever strip by recording the tip deflection under varying weights or masses. A digital scale with high accuracy was used to measure the mass. Masses were placed onto the cantilever strip incrementally and the corresponding strain gauge output signals were monitored and recorded. The calibration results are shown in Fig. 2.

2.6 Derivation of falling velocity and terminal velocity

The waterdrop test uses a hypodermic needle (equivalent 4.0 mm drop diameter) to generate an artificial rainfall. From Fig. 3, momentum was first derived based on calculated velocity of cantilever spring, v_s, which is derived from the conversation of energy immediately after the impact and the end of impact. The equation is as follows:

From the principle of energy conservation for spring system:

$$\frac{1}{2}(m+M)v_s^2 = \frac{1}{2}K\delta^2 \quad [1]$$

where *m* is mass of a waterdrop (g), *M* is mass of impact pad (g), *K* is stiffness of the cantilever strip at the loading point, and δ is deflection at the loading point or free-end tip of the cantilever strip. Rearrange Eq. [1], v_s can be expressed as:

$$v_s = \left(\frac{K}{m+M}\right)^{\frac{1}{2}}\delta \quad [2]$$

From the principle of conservation of momentum, *P*, before and after the impact of raindrop, total initial momentum is equal to total final momentum.

The following equation is obtained:

$$P_{initial} = P_{final}$$

$$mv = (m+M)v_s \quad [3]$$

Substituting v_s from Eq. [2] to Eq. [3], the following velocity equation is derived:

$$v = \left[K\left(1+\frac{M}{m}\right)\right]^{\frac{1}{2}}\delta \quad [4]$$

By substituting the spring stiffness *K*=0.0091 (N/mm) and *M*=1.43 (g), the final velocity equation is obtained as follows:

$$v = 0.095\left(1+\frac{1.43}{m}\right)^{\frac{1}{2}}\delta \quad [5]$$

2.7 Derivation of rainfall impact force

Impact force of a simulated waterdrop was directly derived by the output signal of the strain gauges. The miniature strain gauges were mounted to the top and bottom sides of the copper-alloy cantilever strip near the clamping end. The strip size was 50 mm (length), 4.0 mm (width) and 0.2 mm (thickness). A light and circular concave impact pad was placed on the tip of the strip vertically by a frictionless pin. When a raindrop strikes the impact pad, the cantilever strip experienced a deflection and the strain gauge sensor picked up the surface strain signal. The deflection at the tip of the cantilever strip is proportional to the concentrated force applied. Maximum deflection of the strip at the tip can be expressed structurally by Eq. [6].

$$F = K\delta = \frac{3EI}{L^3}\delta \quad [6]$$

where *F* is force (N), *L* is length of cantilever (mm), *E*: modulus of elasticity of a material, *I* is moment of inertia, *EI* is stiffness of the strip at the loading point, and δ is deflection at the loading point (mm). Equivalent of the cantilever spring's stiffness $K = 3EI / L^3$ or slope of the graph between the weight and the deflection (*K*=0.0091 N/mm) in Fig. 2.

3. Results and discussions

3.1 Measurement of velocity of a waterdrop with heights

In the beginning, the strain gauge was calibrated against deflection and mass to construct a relationship and graph and equations of the calibration were obtained. During calibration against falling waterdrop with varying height, the output of the strain gauge was calibrated against height of a falling waterdrop with predetermined size and mass. Indoor building stair, which is surrounded by a wall and closed to direct moving air, was used an elevation for changing height for waterdrop. Falling height varies with number of staircase and was calibrated less than 18 m. A drop was formed by using a rain simulator and allowed to fall freely from height. After a falling waterdrop with known mass and size collided with the impact pad of the device, the impact pad underwent a deflection and strain gauge sent analog output signal to the data recorder before the signal is digitized and displayed a waveform. The vibrating waveform showed the amplitude or peak deflection with known time, which can be viewed by software provided by the company.

Manual measurement of the peak and time of the signal is recorded. By using a principle of momentum conservation and energy conservation, velocities of waterdrop were obtained. With known mass, size, and velocity, a relationship between height and velocity of falling waterdrop was obtained. In addition, momentum from the falling waterdrop can be directly obtained. Experimental data from Laws (1941) were used for comparison with the measured data.

The derived equation for falling velocity, Eq. [5] is a function of two different physical properties: mass, *m*, is a property of rainfall, and deflection, δ, is a property of cantilever. However, a single property whether *m* or δ can also be incorporated to *Eq.* [5]. This can be achieved by

using the calibration results in Fig. 2, where *m* is linearly proportional to δ by a factor of 0.925.

Results in Fig. 4 demonstrate the reliability of the instrument as the measured data from this study was comparatively in good agreement with the measured data from Laws (1941). The output from the strain gauge sensor was captured at a rate of 5 μs at a frequency of 30 Hz. The rise time of the signal to the peak can be reliably used to derive the velocity. The measured data was fitted by a hyperbolic relationship as shown in the graph.

3.2 *Relationship of strain gauge output to momentum and kinetic energy*

It is commonly practice that kinetic energy (*KE*) of rainfall event or storm is derived in relation to rainfall intensity (*RI*). For example, Onaga et al. (1988) introduced relationship for *KE* and *RI* in Okinawa prefecture of Japan as *KE*=0.098+0.106log (*RI*). In this study, kinetic energy (*KE*) of a drop of water was calculated from $KE=0.5mv^2$. Assuming the validity of Eq. [5], smooth experimental data for terminal velocity and masses or equivalent drop diameters from Gunn and Kinzer (1949) were used for analysis to obtain rainfall erosivity and impact forces. Under natural conditions, if DSD or individual drop size is available, *KE* of initial waterdrop can be determined. The overall *KE* of rainfall event also can be derived based on summation of *KE* of individual drop sizes. Detail of this method can be explained by Abd Elbasit et al., 2015,

Figure 5 showed the result of the derived correlation between the output of strain gauges and estimated kinetic energy. Relationship between the estimated momentums was also established. It was found that relationship of momentum and kinetic energy was linear to the strain gauge output, whereas the equivalent diameters of waterdrops were related to the strain gauge output by a cubic root.

3.3 *Relationship of terminal velocity and impact force to drop mass*

The impact force of waterdrops for various sizes was estimated by assuming the validity of Eq. [5]. The smooth

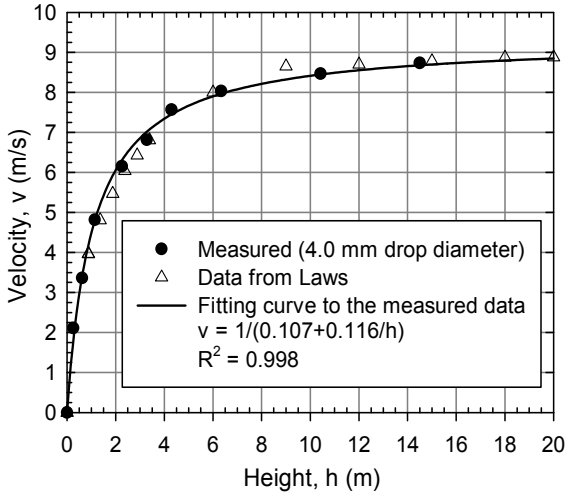

Fig. 4. Measurement of velocity with heights for a 4.0 mm diameter waterdrop.

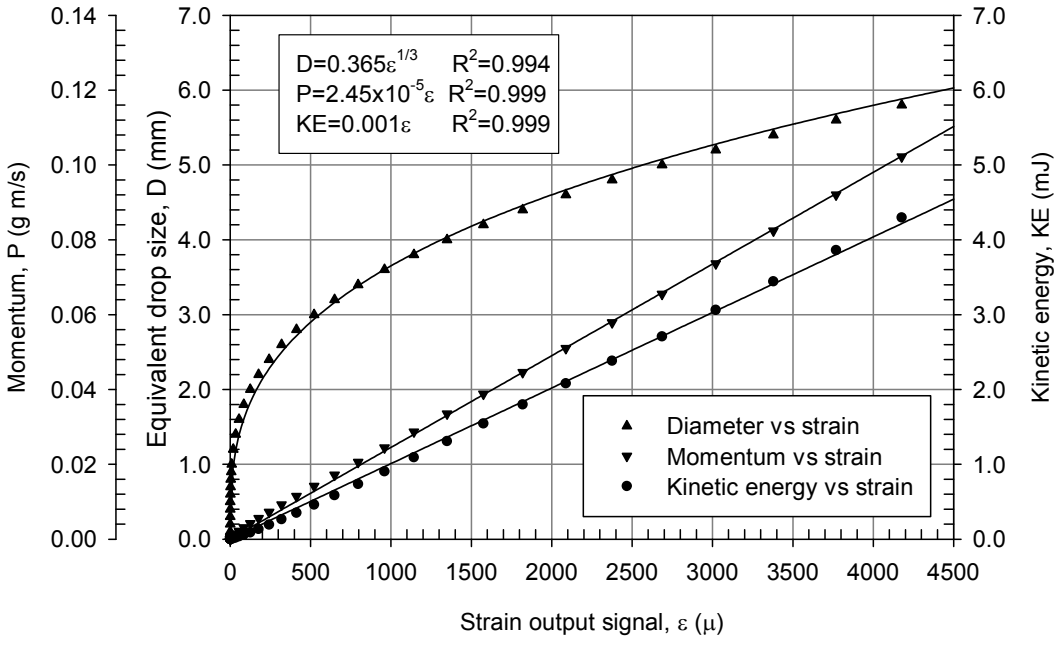

Fig. 5. Relationship of strain gauge output to momentum and kinetic energy.

data for terminal velocities for varying masses of drop sizes from experiments of Gunn and Kinzer (1949) were also used for analysis because these data are the most comprehensive, well-known and reliable data literature. Figure 6 shows the result of the derived correlation of the terminal velocities and impact forces as functions of the mass of varying drop sizes. Relationship between the estimated impact forces to the drop masses was found to be a linear by the best fitted line as shown in the figure. The linearity can be further reinforced by the explanation of the derived equation of impact force in Eq. [6], where impact force, *F*, is linearly proportional to the output of the strain gauges or deflection at the loading point of the cantilever strip by a constant or the cantilever stiffness, *K*, at the loading point, where *K* is equal to 0.0091 (N/mm) as calculated from the calibrated result of the weight, and the deflection, in Fig. 2. The data of terminal velocity as a function of drop mass from Gunn and Kinzer (1949) were also best fitted with an exponential function as shown in Fig. 6. The results from Gunn and Kinzer (1949) represent the upper bound limit (Goebes et. al., 2014) and approximately on average (Raupach and Berne, 2015) for the relationship between drop size distribution and drop-size velocity under natural conditions. Similarly, relationship between the impact forces to varying sizes of waterdrop also was obtained as shown in Fig. 7, where the data were best fitted with similar exponential function to the best fit curve shown in Fig. 6. However, relationship between impact forces to the drop diameters was found to follow a power law. The impact force shows the maximum magnitude at 80 mN, corresponding to the drop diameter of 6.0 mm. Under natural conditions, if the drop size distribution (DSD) of rain is known, the impact forces can thus be computed.

Results of the impact forces in this study were obtained similar to the experiment results conducted by Soto et al. (2014), with one order of difference. In comparison, the impact force results using piezoelectric sensor from Nearing and Bradford (1986) showed a disparity by two order of difference to this experiment data. Patterns of impact force of a single drop size on a solid surface could also yield different results from actual soil surface where the soil surfaces of different soils are characterized by different roughness and frictional angles. In addition, subsequence waterdrops or rain also constitute to the discrepancy of the results. Angles of falling waterdrops is also another behavior that needed to be accounted for when dealing with actual rainfall, which mostly influenced by ambient conditions such as wind speed, relative humidity, drag force, air density, temperature, and specific density of rain. However, the results from this study are imperative that output from the strain gauges can be used to determine the velocities and impact forces.

4. Conclusions

This research was focused on the preliminary laboratory experiment for assessment of rainfall erosivity and impact forces for splash erosion study with consideration of modeled drop sizes and velocities from literature data. Under consideration of cost, maintenance, sampling, installation and mobilization constraints, a portable device developed in this study was found to be a simple and new potential instrument for continuously and automatically measuring the dynamic properties (kinetic energy, velocity, momentum, impact force) of a falling waterdrop. The equations for the falling velocity and its impact force of a waterdrop were derived based on the strain outputs. In addition, the equations were employed

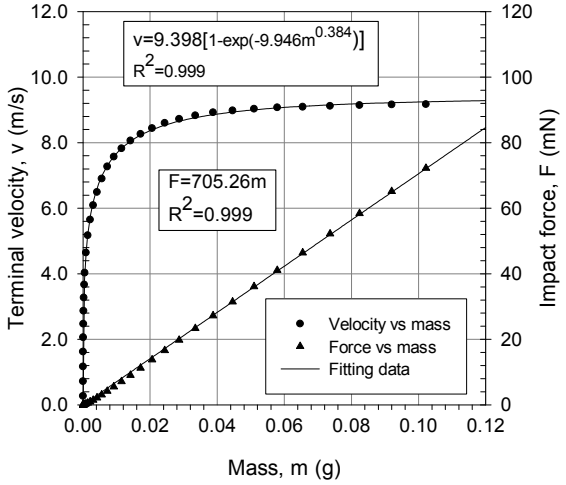

Fig. 6. Relationship for terminal velocities and impact forces to drop diameters.

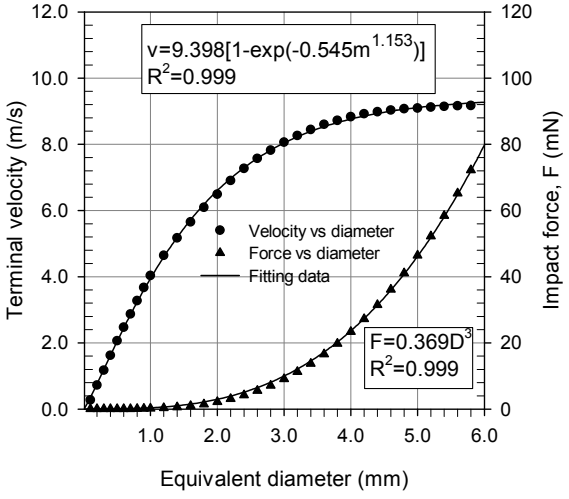

Fig. 7. Relationship for terminal velocities and impact forces to drop diameters.

to derive the terminal velocities and corresponding impact forces as a function of waterdrop diameters.

This research was validated by a single size of waterdrop for estimating terminal velocity, momentum, kinetic energy, and impact force. Variability and reliability of drop size diameters is needed for further comparison with natural rainfall data in the field. Advanced development of the strain-gauge based sensor could also be further developed as a disdrometer for measuring meteorological or hydrological parameters that are not commonly available for soil erosion study. For example, velocity and drop size distribution derived from measured deflection of the tip of cantilever or measured impact force could be readily derivable. This could be enhanced by developing a computer algorithm for obtaining the drop size distribution.

Acknowledgements

This research was carried out under the scholarship supported by the Ministry of Education, Culture, Sports and Technology of Japan and Grant-in Aid for Scientific Research No.24656287, led by Prof. Noriyuki Yasufuku. Special thanks to Mr. Michio Nakashima from geotechnical laboratory of Kyushu University for his technical supports.

References

Abd Elbasit, M.A., Yasuda, H. and Salmi, A., 2011. Application of piezoelectric transducers in simulated rainfall erosivity assessment. Hydrological Sciences Journal, **56**(1):187-194.

Abd Elbasit, M.A., Ojha, C.S.P., Ahmed, Z., Yasuda, H., Salmi, A., and Ahmed, F., 2015. Rain microstructure and erosivity relationships under pressurized rainfall simulator. Journal of Hydrological Engineering, ASCE, **20**(6): C6015001-1 to 6015001-6.

Bates, B.C., Kundzewicz, Z.W., Wu, S., and Palutikof, J.P., 2008. Climate Change and Water. Technical Paper of the Intergovernmental Panel on Climate Change, IPCC Secretariat.

Camici, S., Brocca, L., Melone, F., and Moramarco, T., 2014. Impact of Climate Change on Flood Frequency Using Different Climate Models and Downscaling Approaches. J. Hydrol. Eng., ASCE, **19**(8).

Carollo, F.G. and Ferro, V., 2014. Modeling rainfall erosivity by measured drop-size distributions. Journal of Hydrological Engineering, ASCE, C4014006-1 to C4014006-7.

Cousino L.K., Becker R.H., and Zmijewski K.A., 2015. Modeling the effects of climate change on water, sediment, and nutrient yields from the Maumee River watershed. Journal of Hydrology, **4**: 762–775.

Crozier, M.J., 2010. Deciphering the effect of climate change on landslide activity: A review. Geomorphology, Elsevier, **124**(3-4):260-267.

Hinkle, S.E., 1989. Water drop kinetic energy and momentum measurement considerations. Applied engineering in agriculture, American Society of Agricultural Engineers, **5**(3): 386-391.

IPCC, Intergovernmental Panel on Climate Change., 2012. Managing the risks of extreme events and disasters to advance climate change adaptation. Special Report of the IPCC.

Goebes, P., Seitz, S. Geibler, C. Lassu, T., Peters, P., Seeger, M., Nadrowski, K., and Scholten, T., 2014. Momentum or kinetic energy – How do substrate properties influence the calculation of rainfall erosivity?. Journal of Hydrology, Elsevier, **517**: 310-316.

Gunn, R. and Kinzer, D.G., 1949. The terminal velocity of fall for water droplets in stagnant air. Journal of Meteorology. **6**: 243-248.

Jayawardena, A.W. and Rezaur, R.B., 2000. Measuring drop size distribution and kinetic energy of rainfall using a force transducer. Hydrological Processs, John Wiley & Sons, **14**:37-49.

Laws, O.J., 1941. Measurements of the fall velocity of water-drops and raindrops. Hydrology. Transactions, American Geophysical Union. **22**: 709-721.

Meshesha, D.T., Tsunekawa, A., Tsubo, M., Haregeweyn, N. and Tegegne., 2015. Evaluation of kinetic energy and erosivity potential of simulated rainfall using laser precipitation monitor. Catena, Elsevier, **137**: 237-243.

Nearing, M.A. and Bradford, J.M., 1986. Relationship between waterdrop properties and forces of impact. Soil Sci. Soc. Am. J, **51**:425-430.

Nearing, M.A., Bradford, J.M., & Holtz, R.D., 1986. Measurement of force vs time relations for waterdrop impact. The Soil Science Society of American Journal, **50** (6): 1532-1536.

Nearing, M.A., Pruski, F.F., and O'Neal, M.R., 2004. Expected climate change impacts on soil erosion rates: A review. Journal of Soil and Water Conservation, **59**(1): 43-50.

Onaga, K., Shirai, K. and Yoshinaga, A. (1988). Rainfall erosion and how to control its effects on farmland in Okinawa. In Rimwanich, S. (ed.), Land conservation for future generations. Department of Land Development, Bangkok: 627–39.

Rahardjo H., Nio S.F., Harnas, F.R., Leong E.C., 2014. Comprehensive instrumentation for real time monitoring flux boundary condition in slope. Procedia Earth and Planetary Science, Elsevier, **9**: 23-43.

Raupach, T.H., and Berne, A., 2015. Correction of raindrop size distributions measured by Parsivel disdrometers, using a two-dimensional video disdrometer as a reference. Atmos. Meas. Tech., **8**: 343–365.

Sharma, P. P., 1996. Interrill erosion, in Agassi, M. (Ed.), Soil Erosion Conservation and Rehabilitation. Marcel Dekker, New York, 125-152.

Shrestha, B., Babel, M.S., Maskey, S., Griensven, A.V., Uhlenbrook, S., Green, A., and Akkharath, I., 2013. Impact of climate change on sediment yield in the Mekong River basin: a case study of the Nam Ou basin, Lao PDR. Hydrol. Earth Syst. Sci., **17**: 1–20.

Soto, D., Lariviere, D.B.A., Boutillon, X., Clanet, C. and Guere, D., 2014. The force of impacting rain. The Royal Society of Chemistry, **10**: 4092-4934.

Wischmeier, W.H. and Smith, D.D., 1978. Predicting rainfall erosion losses - A guide to conservation planning. USDA, Handbook No. 537.

Yasufuku, N., Araki, K., Omine, K., Okumura, K., & Iwami, K., 2015. Evaluation of inhibitory effect by adaptation measures for red soil runoff from farmland due to heavy rainfall. Journal of Disaster Research, **10 (3)**, 457-466.

Symbols and abbreviations

F	Impact force due to a waterdrop
m	Mass of raindrop or waterdrop
M	Mass of impact pad
v	Velocity of waterdrop
v_s	Velocity of cantilever spring
ε	Strain gauge output
δ	Deflection at the tip of a cantilever strip
L	Length of span of a cantilever strip
E	Modulus of elasticity
I	Moment of inertia
P	Momentum
K	Stiffness of an equivalent spring
KE	Kinetic energy
RI	Rainfall intensity
D	Diameter of a waterdrop
exp()	Exponential e
h	Height of a falling waterdrop
H	Weight of a waterdrop